The construction and performance of honeycomb strip chambers

van Apeldoorn, G.W.; Daum, C.; van de Graaf, H.; Linde, F.L.; Massaro, G.G.G.; Bakker, F.; Colijn, A.P.; Groenstege, H.; Rewiersma, P.; Sman, S.; Tolsma, H.P.T.; Bergman, R.; Brouwer, C.; Dijkema, J.; Koenig, A.; Wijnen, T.

DOI
10.1016/0168-9002(95)00084-4

Publication date
1995

Published in
Nuclear Instruments & Methods in Physics Research Section A - Accelerators Spectrometers Detectors and Associated Equipment

ELSEVIER

Nuclear Instruments and Methods in Physics Research A 360 (1995) 60-66

NUCLEAR INSTRUMENTS & METHODS IN PHYSICS RESEARCH Section A

The construction and performance of honeycomb strip chambers

G. van Apeldoorn [a], F. Bakker [a], A.P. Colijn [a], C. Daum [a], H. van der Graaf [a], H. Groenstege [a], F. Linde [a], G. Massaro [a], P. Rewiersma [a], S. Sman [a], H. Tolsma [a,*], R. Bergman [b], C. Brouwer [b], J. Dijkema [b], A.C. König [b], T. Wijnen [b]

[a] *NIKHEF-H, Kruislaan 409, 1098 SJ Amsterdam, The Netherlands*

[b] *University of Nijmegen, Toernooiveld 1, 6525 ED Nijmegen, The Netherlands*

Abstract

This paper gives an overview of all honeycomb strip chambers constructed so far. The method of construction is described, and results from a beam test and cosmic rays are presented.

1. Introduction

The Honeycomb Strip Chamber (HSC) was developed for the muon spectrometers of the LHC and SSC experiments [1]. They consist mainly of folded foil: two foils together form a layer of hexagonal tubes. By putting a thin wire in the centre of the cells, drift tubes are formed. Conductive strips on the foils allow the measurement of a second coordinate from the distribution of the induced charge. The HSC combines low costs with a high-precision two-coordinate readout and an extremely low scattering mass. The application of HSCs is therefore considered in B-physics experiments like HERA-B [2].

The chambers are summarised in Table 1. In this paper, their construction is described, followed by a section concerning their performance.

* Corresponding author.

Table 1
Characteristics of the HSC prototypes

Characteristics	P1	TRACAL	P2	P3	P3A
Year	1990	1991	1992/93	1993	1994
No. constructed	1	25	3	1	1
No. wires/layer	24	48	255	8	8
No. strips/layer	54	192	192	-	-
No. layers/chamber	8	1	8	8	8
Outer cell radius (mm)	5.77	5.77	5.77	11.54	11.54
Wire length (m)	0.3	1.0	1.0	5.7	5.7
Wire diameter (μm)	20/30	30	30	50	50
Wire pitch (mm)	12.7	12.7	12.7	25.4	25.4
Strip length (m)	0.3	0.6	3.2	-	-
Strip pitch (mm)	5.08	5.08	5.08	-	-
Plane pitch (mm)	10.7	-	10.64	20.0	20.0
Folded insulating foil	kapton	melinex	mylar	mylar	-
Thickness (μm)	100	75	75	75	-
Flat insulating foil	kapton	mylar	mylar	kapton	-
Thickness (μm)	100	75	75	100	-
Folded conductor	copper	copper	copper	copper	aluminium
Thickness (μm)	17	0.3	0.8	0.8	50
flat conductor	-	-	-	copper	aluminium
Thickness (μm)	-	-	-	17	50

2. Chamber construction

2.1. The "Prototype 1" (P1) chamber

This chamber was made from kapton/copper laminated foil. The strip pattern was etched using standard flexible printed circuit board technology [3]. A precision of 0.1 mm on the position of the strip edges was obtained. The foils

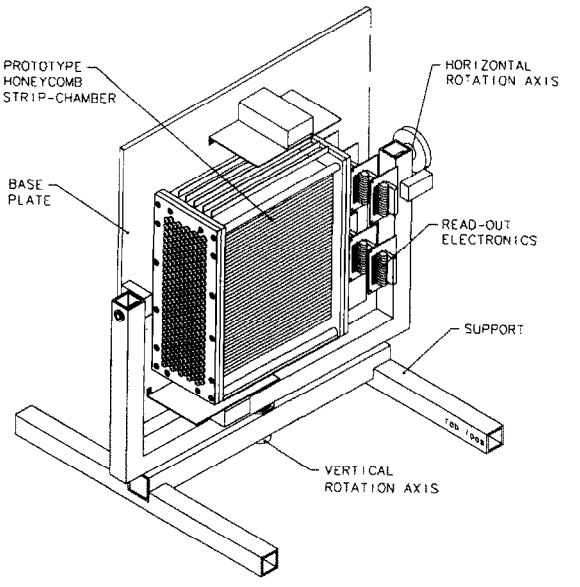

Fig. 1. The P1 chamber and its support.

SSDI 0168-9002(95)00084-4

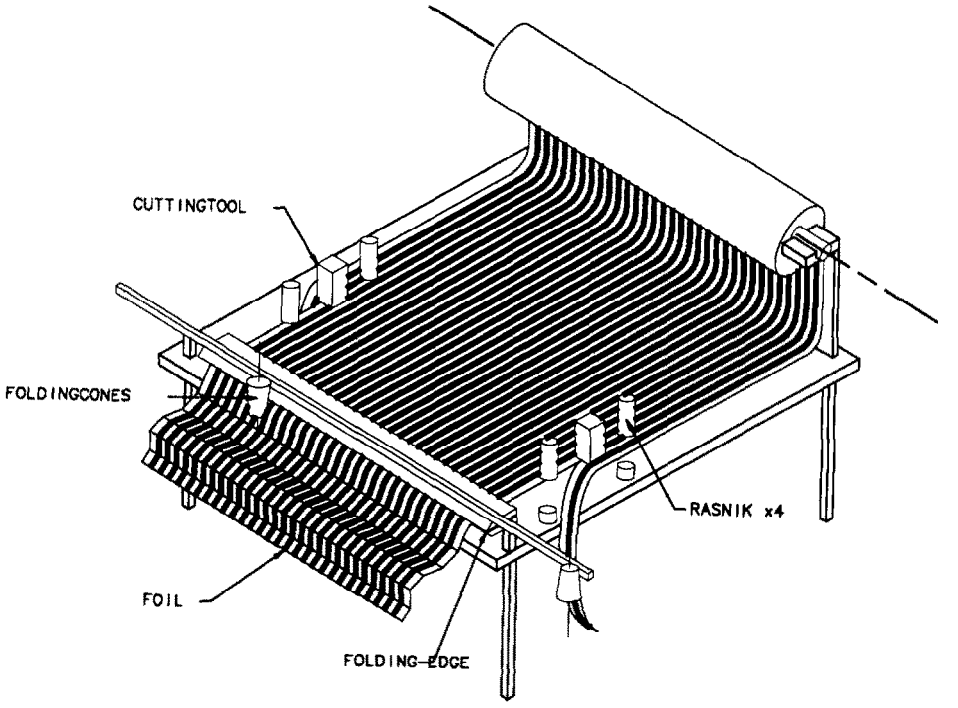

Fig. 2. Machine used to fold mylar foils.

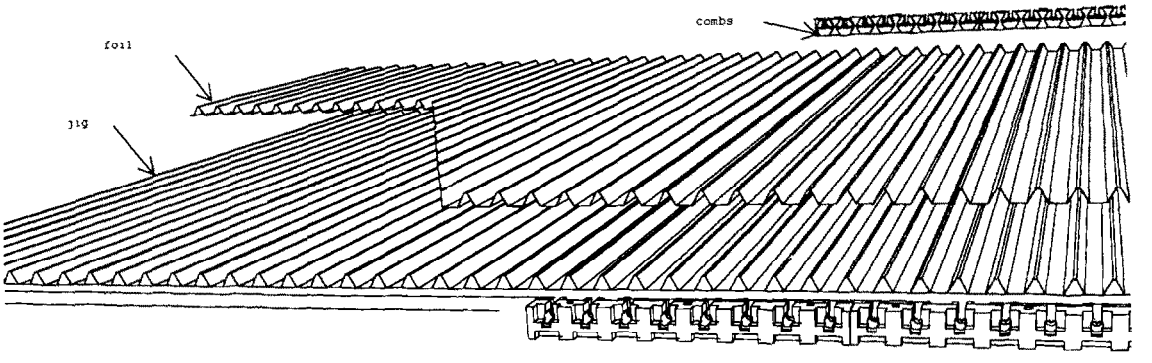

Fig. 3. Schematic assembly of a monolayer: foil-template and end-combs are shown.

(flat dimensions $400 \times 600\,mm^2$) were folded by means of a template. The foil was fixed in the template by bolting half-hexagonal bars onto each half cell of the template, starting from one side. The template was then put in an oven and heated at 305°C for 30 minutes. The thermo-plastic properties of kapton foil were such that the foil kept its "ribbon" shape. Two templates were made to hold a ribbon foil in position by applying a vacuum. Araldite was applied on the narrow flat area between two cells. Then the templates with the foils were placed facing each other. After the glue had hardened, one template was removed. A flat kapton foil (without copper) was then glued onto the cell layer, forming a monolayer stiff enough to be handled. At each cell-end a nylon plug was inserted. The nylon plugs fitted into an aluminium gas distribution box in which the wires were fixed. The completed chamber was fixed onto an aluminium base plate supported by a stand which allowed the chamber to rotate over two angles (see Fig. 1).

2.2. The TRACAL chambers

The construction of these chambers is described in detail in Ref. [4].

2.3. The "Prototype 2" (P2) chambers

These chambers were constructed in order to study the strip readout in the case of long strips (3.25 m) and to gain experience with building large HSC units. Given the larger length of the foils (5 m), the perpendicularity between the folds and the strips had to be even better than for the TRACAL chambers. This was achieved by active stabilisation of

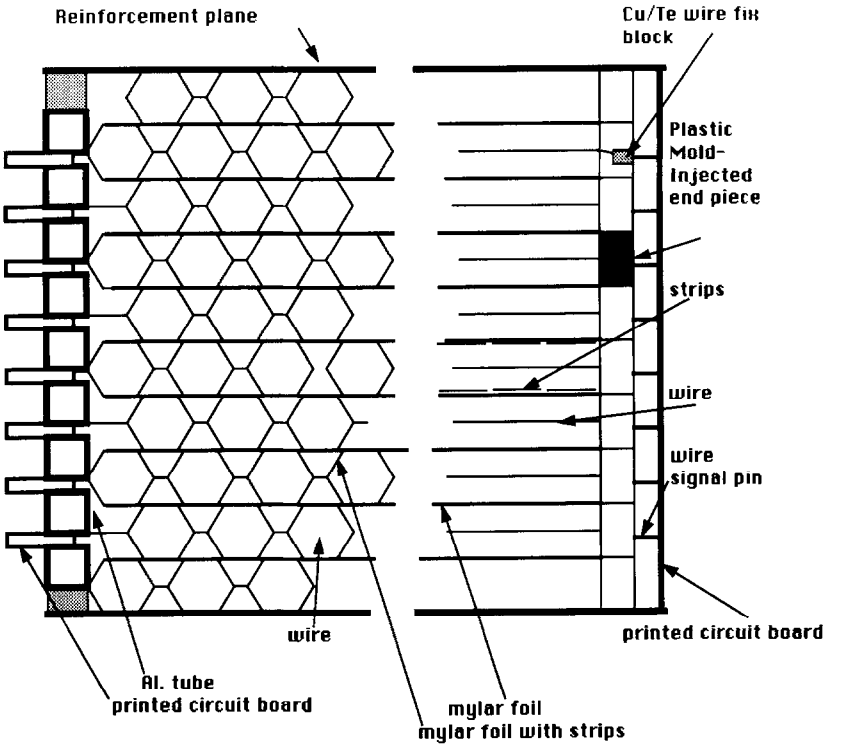

Fig. 4. Cross-sections of a multilayer. Left: perpendicular to the wires. Right: perpendicular to the end-combs.

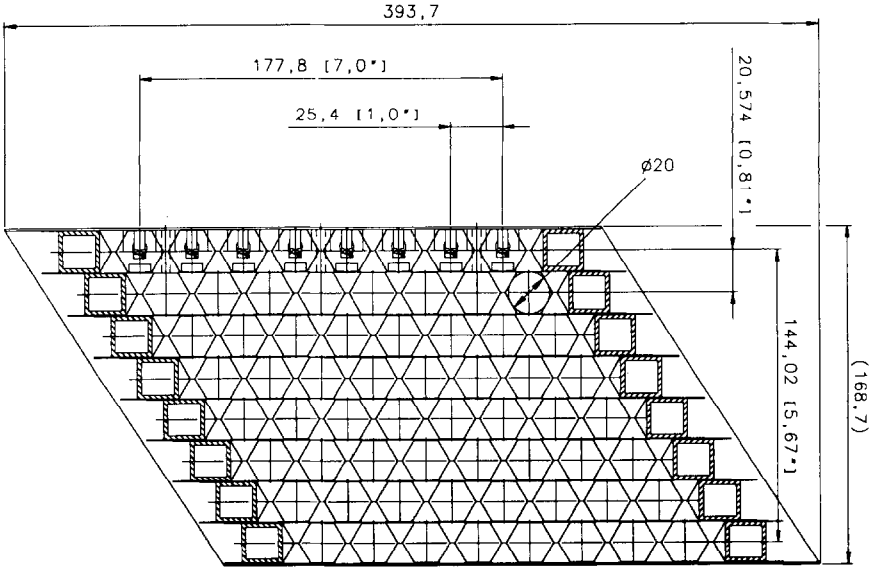

Fig. 5. Cross section of the P3 chamber.

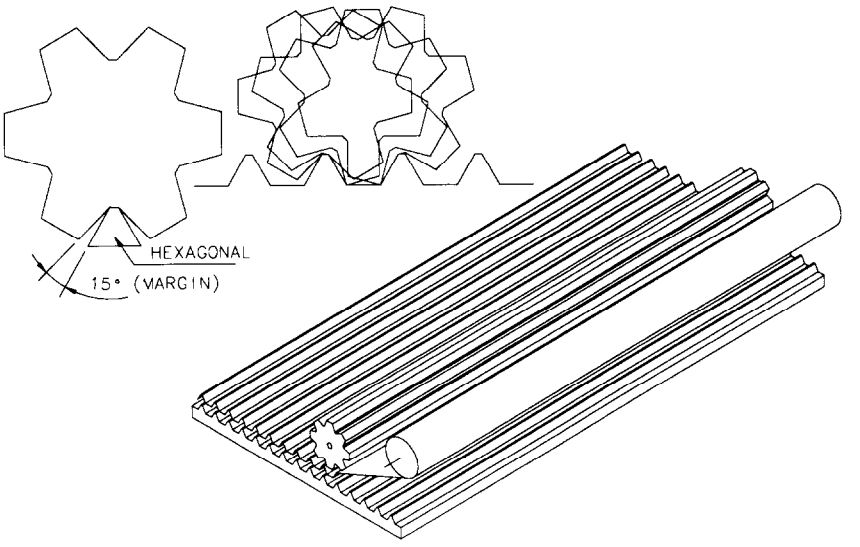

Fig. 6. Reel and template used to fold aluminium foils.

the foil position on the folding machine. The foil transport mechanism, previously made up of two pneumatically driven shuttles, was replaced by two high-precision linear motors with a step resolution better than 1 μm. The position of the foil was monitored by four RASNIK systems [5] which effectively measured the angle between the folding edge and the strips, as well as the translation of the foil perpendicular to the strips (see Fig. 2).

A folded foil was put on a template and a vacuum was applied (see Fig. 3). Then, at the cell edges, mold-injected precision plastic "Lego" blocks were glued on the foil; the blocks were positioned by pins on the template. The blocks had an 8-fold hexagonal shape at one side to define the foil geometry at the chamber edge. On the other side, Cu/Te blocks with a slit in which a wire could be fixed by crimping [6], were glued. All the wires of a monolayer were fixed before the top foil was applied.

The top foil was positioned by a second (full-scale) template which was lowered on the bottom template. The foils were fixed together by means of ultrasonic welding. Over the course of one night, all 6000 welding spots of one monolayer were applied automatically. The top template was then lifted from the bottom template, and a flat foil was glued onto the cell layer. An auxiliary frame was mounted on the monolayer, which was then removed from the bottom template, while keeping its shape due to the stiffness of the frame.

The chamber was assembled by fixing the first monolayer onto a flat aluminium table. Then the next monolayer (kept in shape by the auxiliary frame) was glued onto the previous one. After the 8th monolayer, the chamber was covered on both sides with an aluminium sheet (0.5 mm) to provide for stiffness and shielding.

At the "Lego" block sides of the chamber, printed circuit boards were mounted with pins sticking in the holes of the Cu/Te crimping blocks (see Fig. 4). These boards act as gas seal, HV distributors and signal feedthrough. The space between the boards and the "Lego" blocks serve as a gas distributor. By placing the gas input and output diagonally on the chamber, a homogeneous flow through the cells was obtained.

See Ref. [7] for a detailed description of the P2 chambers.

2.4. *The "Prototype 3" (P3) chamber*

The P3 chamber (see Fig. 5) has a wire length of 5.5 m, and a cell radius twice as large as the previous chambers. It has a middle wire support to limit the distance between the wire position and the cell axis. The width of the chamber was limited to eight cells for reasons of economy. The foil was folded on the same machine as used for the P2 chambers: the linear motors were computer controlled so the geometry of the ribbon foil is programmable. The construction of the monolayers was similar to the P2 chambers. The top and bottom templates were made by an industrial firm. Two ribbon foils were glued together, instead of ultrasonic welded. As flat foil a kapton–copper laminate was chosen in order to limit crosstalk between two monolayers. Since the second coordinate was not required, all strips were connected to ground at the chamber edge.

2.5. *The "Prototype 3 Aluminium" (P3A) chamber*

The geometry of the chamber was identical to the P3 chamber. If a second coordinate is not needed, aluminium foil has the advantages that it is much cheaper than the sputtered or laminated foils and it can be folded simply by rolling a reel over the bottom template (see Fig. 6).

3. Chamber performance

3.1. The "Prototype 1" (P1) chamber

Details of the performance concerning the strip readout have been published before [3]. The readout of the wires was tested with cosmic rays and in beam tests at the RD5 experimental test site, CERN, Geneva.

Fig. 7 shows a reconstructed track: the cosmic ray tests showed that the hexagonal tube worked well as a proportional drift tube (see Fig. 8). To investigate the performance of HSCs inside a magnetic field, the P1 chamber was positioned in the 3 T EHS magnet in RD5. The magnetic field orientation was perpendicular to the incident particles and parallel to the wires. Measurements were done with several values of the magnetic field. The measurements show excellent behaviour of the multi-layer HSC inside a magnetic field, even at 3 T (see Fig. 9). The spatial resolution is maintained despite a change in the relation between the drift distance (r) and drift time (t) due to variation of the magnetic field strength, causing a variation in the path length of the drifting electrons.

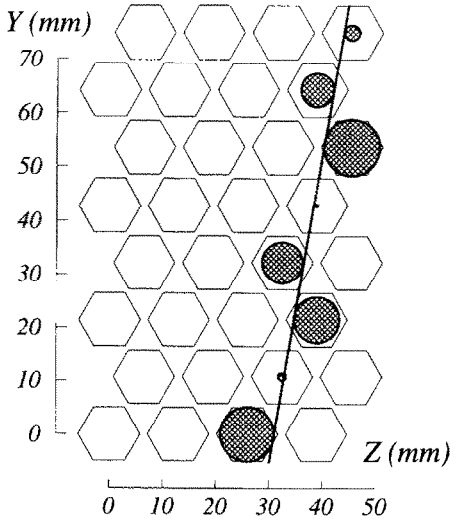

Fig. 7. Example of a reconstructed HSC track. The circles represent the measured drift distances to the anode wire.

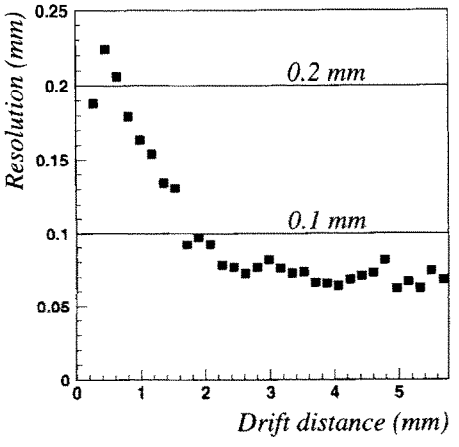

Fig. 8. Single wire resolution measured with cosmic rays in P1. The gas mixture was 50 % Ar and 50 % CO_2; HV = 2100 V, wires: 20 μm diameter.

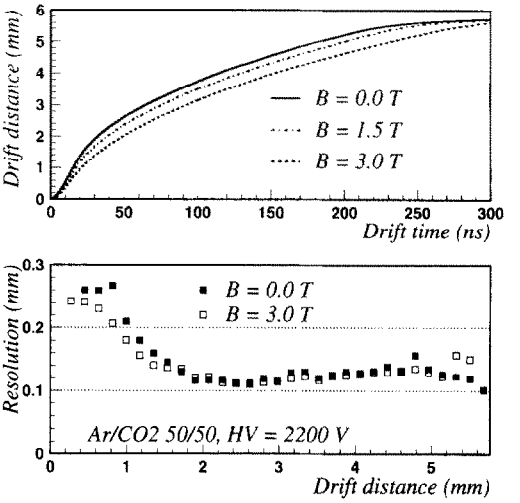

Fig. 9. Top: the drift distance (r) as function of drift time (t) for different values of the magnetic field parallel to the anode wires. Bottom: the resolution as function of drift distance for 0.0 and 3.0 T fields. The change in the r–t characteristics has been taken into account.

The r–t relation is calculated by the autocalibration method. Residuals are calculated in slices of drift distance for a data sample of typically 5000 events. The shift of the mean value in the residuals of each slice gives the correction to be applied to the initial r–t relation (Fig. 10, top-right). Since there are no external track defining points, the fit of the track depends only on the erroneous r–t relation. The final r–t relation can, therefore, be found by repeating the procedure several times. Initial and final (15 iterations) r–t relation are shown in Fig. 10 (left) for a data sample taken with cosmics. The initial curve has the form r = const. $\times \sqrt{t}$. Clearly, the spatial resolution improves whenever a more realistic r–t relation is used (Fig. 10, bottom-right). Only one r–t relation is used for all 96 wires.

3.2. The TRACAL chambers

Detailed results have been published before [4,8].

3.3. The "Prototype 2" (P2) chambers

Three P2 chambers were put in the RD5 muon beam as shown in Fig. 11. The geometry of the three chambers is an image of a "muon tower" in which the four corners of each of the three chambers line up with the origin of the muon track [1]. With this, the track sagitta S can be measured ($S = Z_2 - \frac{1}{2}(Z_1 + Z_3)$ from the $Z_{1,2,3}$ coordinates obtained from the drift time data). The relative position of the middle

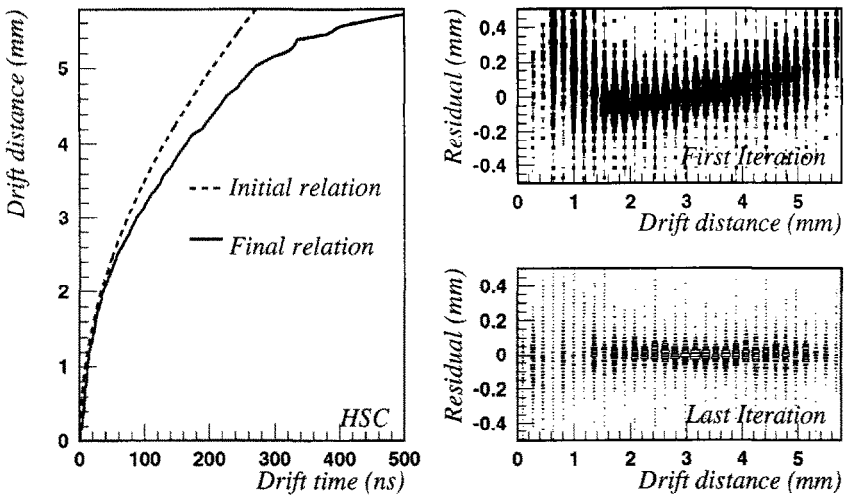

Fig. 10. Left: initial and final r–t relation. Right: residuals in slices of the position in the cell before (top) and after (bottom) autocalibration.

chamber with respect to the outer two was monitored by means of six RASNIK/CCD systems [9].

The analysis of the data is still in progress, but preliminary results show a spatial resolution of the strips of better than 85 μm. The spatial resolution obtained with the wires depends on the type of electronics used. Under experimental conditions similar to the P1 tests, the results are equal to that of the small prototype. The preliminary result for the measured error in S is 93 μm (see Fig. 12).

In order to compare the relative chamber position with the sagitta measured from the muon tracks, the middle chamber was moved along the X, Y and Z axes and also rotated over these axes. The analysis of this data is in progress [7].

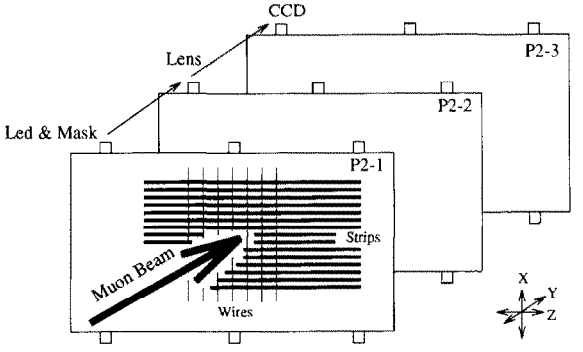

Fig. 11. Setup of the RD5-P2 experiment.

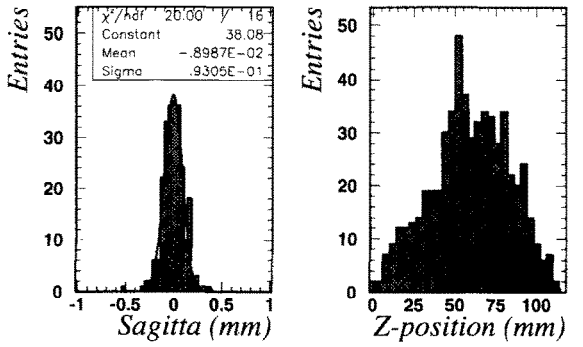

Fig. 12. Left: sagitta measured with the P2 chambers in the absence of a magnetic field. Right: beam profile of the RD5 muon beam (200 GeV) in the first chamber.

3.4. The "Prototype 3" (P3) chamber

P3 has been tested with cosmic rays and recently in the RD5 muon beam. Results of the cosmic ray tests are presented in Fig. 13. Several gases have been used to find one with an acceptable maximum drift time and with a good spatial resolution. The final choice of the drift gas depends on the specific requirements of the experiment in which the HSC is applied. The analysis of the data is in progress.

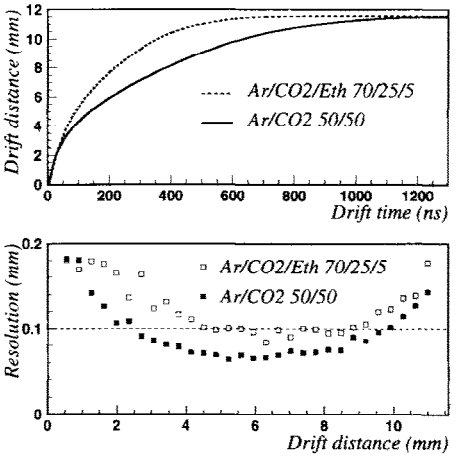

Fig. 13. Top: the drift distance (r) as function of drift time (t) for two different gasses. Bottom: the resolution as a function of drift distance for both gasses.

Acknowledgements

We would like to thank J. Buskens, G. Evers, H. Schuylenburg and their groups for their creative and fruitful contributions.

References

[1] F. Bakker et al., Honeycomb Strip Chambers for the ATLAS Muon Spectrometer, ATLAS MUON-NO-035, CERN (1994).
[2] HERA-B, An Experiment to Study CP Violation in the B System Using an Internal Target at the HERA Proton Ring, DESY-PRC 94/02 (1994).
[3] H. van der Graaf et al., Nucl. Instr. and Meth. A 307 (1991) 220.
[4] F. Bakker et al., Nucl. Instr. and Meth. A 330 (1993) 40.
[5] P. Duinker et al., Nucl. Instr. and Meth. A 273 (1988) 814.
[6] R. Bock et al., Nucl. Instr. and Meth. A 336 (1993) 128.
[7] G. van Apeldoorn et al., The construction of three large honeycomb strip chambers and their performance in a projective alignment tower geometry, to be published in Nucl. Instr. and Meth.
[8] M. Aalste et al., Z. Phys. C 60 (1993) 1.
[9] H. Dekker et al., The RASNIK/CCD 3-dimensional alignment system, Proc. 3rd Conf. on Accelerator Alignment, CERN/Annecy, October 1993, p. 147.